

AgentMixer: Multi-Agent Correlated Policy Factorization

Zhiyuan Li¹, Wenshuai Zhao¹, Lijun Wu², Joni Pajarinen¹

¹Department of Electrical Engineering and Automation, Aalto University

²School of Computer Science and Engineering, University of Electronic Science and Technology of China

{zhiyuan.li, wenshuai.zhao, joni.pajarinen}@aalto.fi, wljuestc@sina.com

Abstract

In multi-agent reinforcement learning, centralized training with decentralized execution (CTDE) methods typically assume that agents make decisions based on their local observations independently, which may not lead to a correlated joint policy with coordination. Coordination can be explicitly encouraged during training and individual policies can be trained to imitate the correlated joint policy. However, this may lead to an *asymmetric learning failure* due to the observation mismatch between the joint and individual policies. Inspired by the concept of correlated equilibrium, we introduce a *strategy modification* called AgentMixer that allows agents to correlate their policies. AgentMixer combines individual partially observable policies into a joint fully observable policy non-linearly. To enable decentralized execution, we introduce *Individual-Global-Consistency* to guarantee mode consistency during joint training of the centralized and decentralized policies and prove that AgentMixer converges to an ϵ -approximate Correlated Equilibrium. In the Multi-Agent MuJoCo, SMAC-v2, Matrix Game, and Predator-Prey benchmarks, AgentMixer outperforms or matches state-of-the-art methods.

Introduction

Cooperative multi-agent reinforcement learning (MARL) has attracted substantial attention in recent years owing to its promise in solving many real-world tasks that naturally comprise multiple decision-makers interacting at the same time, such as multi-robot control (Gu et al. 2023), traffic signal control (Ma and Wu 2020), and autonomous driving (Shalev-Shwartz, Shammah, and Shashua 2016). In contrast to the single-agent RL settings, learning in multi-agent systems (MAS) poses two primary challenges: 1) coordination, that is, agents learning to work together in order to achieve a common goal, and 2) partial observability which limits each agent to her own local observations and actions. To address these challenges, the commonly used learning framework called Centralized Training Decentralized Execution (CTDE) (Lowe et al. 2017; Yu et al. 2022) allows agents to access global information during the training phase while during evaluation learned decentralized policies have access only to local information.

Copyright © 2025, Association for the Advancement of Artificial Intelligence (www.aaai.org). All rights reserved.

To enhance coordination, one line of research is to use value decomposition (VD). VDN (Sunehag et al. 2017) and QMIX (Rashid et al. 2020) learn a centralized joint action value function factorized by decentralized agent utility functions. With the structural constraint of Individual-Global-Max (IGM) (Son et al. 2019), this approach guarantees action consistency between the centralized and decentralized policies. On the other hand, multi-agent policy gradient (MAPG) methods, such as MADDPG (Lowe et al. 2017) and MAPPO (Yu et al. 2022), have achieved high performance. However, even when learning a centralized critic, previous works are still constrained by assuming independence among agents during exploration. Inspired by the Correlated Equilibrium (CE) (Maschler, Zamir, and Solan 2013) in game theory, MAVEN (Mahajan et al. 2019) and SIC (Chen et al. 2022) introduce a hierarchical control method with an external shared latent variable as additional information for agent coordination. Assuming a pre-defined execution order a few recent works further propose autoregressive policies to impose coordination among agents by allowing agents to observe other agents' actions, either explicitly (Wang, Ye, and Lu 2023; Li et al. 2024b) or implicitly (Li et al. 2023; Wen et al. 2022). Most existing correlated policy approaches violate the requirement for decentralized execution. This paper instead aims to achieve a correlated equilibrium in a fully decentralized way which is crucial for real-world applications such as wireless devices (Pajarinen, Hottinen, and Peltonen 2014), where agents are required to operate autonomously while collectively maximizing performance.

In order to mitigate the difficulty of learning under partial observability, CTDE exploits true state information, usually via a centralized critic, to train individual policies conditioned on the local observation-action history. While it is possible to first learn a centralized expert policy and then train the decentralized agents to follow it, it may result in suboptimal partially observable policies since the omniscient critic or agent has no knowledge of what the decentralized agents do not know, referred to as the *asymmetric learning failure* (Warrington et al. 2021). Consider a scenario where two agents of distinct physical shapes try to get to their opposite destinations through two possible paths 1 and 2, as shown in Figure 1. Successful policies should avoid collision as the body sizes of agents always change

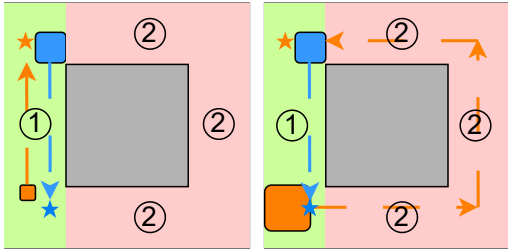


Figure 1: The partially observable bridge crossing task. Two agents (blue and orange boxes), with changing physiques (box sizes) in different episodes as shown in the left and right figures, must navigate to their destinations, marked with stars with corresponding colors, through passageways 1 or 2 while avoiding congestion. The expert is conditioned on an omniscient state indicating the physiques of all agents, while an agent cannot see the physique of another agent. Naively learning from the full observation expert policy, the agents would never stagger passageways, and instead cross the same passageway directly, incurring congestion.

and each passage only permits two small agents or one big agent. In CTDE, we can learn the optimal fully observable joint policy conditioned on agents' physiques, which would select the shorter path 1 when both agents are small. However, naively learning from such a centralized agent could lead to agents jamming on the same passage, as the partially observable agents cannot access the other agent's body size. In contrast, the optimal partially observable policies should ideally ensure that each agent consistently selects distinct passageways to avoid collision. This *asymmetric learning failure* is a prevalent issue in MARL due to the partial observability nature of MAS. While a few works have studied similar challenges in the context of single-agent RL (Walsman et al. 2023), it is worth noting that this issue within the MARL domain has not been thoroughly investigated to the best of our knowledge.

In this paper, we propose *correlated policy factorization*, dubbed AgentMixer, to tackle the above two challenges and achieve CE among agents in a fully decentralized way. Firstly, we propose a novel framework, named *Policy Modifier* (PM), to model the correlated joint policy, which takes as input decentralized partially observable policies and the state information and outputs the modified policies. Consequently, PM acts as an *observer* from the CE perspective and the modified policies form a correlated joint policy. Further, to mitigate the *asymmetric learning failure* when learning decentralized partially observable policies from the correlated joint fully observable policy, we then introduce a novel mechanism called *Individual-Global-Consistency* (IGC), which keeps consistent modes between individual policies and joint policy while allowing correlated exploration in joint policy. Theoretically, we prove that AgentMixer converges to ϵ -approximate Correlated Equilibrium. Experimental results on various benchmarks confirm its strong empirical performance against current state-of-the-art MARL methods.

Related Work

Modeling complex correlations among agents has been attracting a growing amount of attention in recent years. The centralized training decentralized execution (CTDE) paradigm has demonstrated its success in cooperative multi-agent domain (Lowe et al. 2017; Yu et al. 2022). Centralized training with additional global information makes agents cooperate better while decentralized execution enables distributed deployment.

Value decomposition. Value decomposition methods decompose the joint Q-function into individual utility functions following different interpretations of Individual-Global-Maximum (IGM) (Son et al. 2019), i.e., the consistency between optimal local actions and optimal joint action. VDN (Sunehag et al. 2017) and QMIX (Rashid et al. 2020) decompose the joint action-value function by additivity and monotonicity respectively. QTRAN (Son et al. 2019) and QPLEX (Wang et al. 2021a) introduce additional components to enhance the expressive capability of value decomposition. To enhance coordination, MAVEN (Mahajan et al. 2019) introduces committed exploration among agents into QMIX. Recent works delve into applying value decomposition to actor-critic methods. FACMAC (Peng et al. 2021) and DOP (Wang et al. 2021b) combine value decomposition to compute policy gradient with a centralized but factored critic. FOP (Zhang et al. 2021) and MACPF (Wang, Ye, and Lu 2023) derive joint soft-Q-function decomposition according to independent and conditional policy factorization respectively.

Policy factorization. Existing approaches commonly assume the independence of agents' policies, modeling the joint policy as the Cartesian Product of each agent's fully independent policy (Yu et al. 2022; Zhang et al. 2021; Li et al. 2024a). However, such an assumption lacks in modeling complex correlations as it constrains the expressiveness of the joint policy and limits the agents' capability to coordinate. In contrast, some recent works (Wang, Ye, and Lu 2023; Wen et al. 2022; Fu et al. 2022) explicitly take the dependency among agents by presenting the joint policy in an auto-regressive form based on the chain rule. MAT (Wen et al. 2022) casts MARL into a sequence modeling problem and introduces Transformer (Vaswani et al. 2017) to generate actions. Wang, Ye, and Lu (2023) extends FOP (Zhang et al. 2021) with auto-regressive policy factorization. ACE (Li et al. 2023) transforms multi-agent Markov Decision Process (MMDP) (Littman 1994) into a single-agent Markov Decision Process (MDP) (Feinberg and Shwartz 2012), which implicitly models the auto-regressive joint policy. Despite the merits of the auto-regressive model, the fixed execution order may struggle to generalize different cooperative paradigms. Inspired by Correlated Equilibrium (Maschler, Zamir, and Solan 2013), SIC (Chen et al. 2022) introduces a coordination signal to achieve richer classes of the joint policy and maximizes the mutual information between the signal and the joint policy, which is close to MAVEN. Correlated Q-learning (Greenwald and Hall 2003) generalizes Nash Q-learning (Hu and Wellman 2003) based on CE and proposes several variants to resolve the equilibrium selection problem. Similarly, Schroeder de Witt et al.

(2019) learns a hierarchical policy tree based on a shared random seed. Sheng et al. (2023) learns coordinated behavior with recursive reasoning. However, most existing work focuses on fully observable settings or violates the decentralized execution requirement.

Moreover, existing approaches rarely study the issues arising from the use of asymmetric information (Warrington et al. 2021) in CTDE, that is, the joint fully observable critic or agent has access to information unavailable to the partially observable agents. In this paper, we study how to factorize the correlated joint fully observable policy into decentralized policies under partial observability.

Background

Decentralized Partially Observable Markov Decision Processes

In this work, we model a fully cooperative multi-agent game with N agents as a *decentralized partially observable Markov decision process* (Dec-POMDP) (Oliehoek and Amato 2016), which is formally defined as a tuple $\mathcal{G} = (\mathcal{N}, \mathcal{S}, \mathcal{O}, \mathbb{O}, \mathcal{B}, \mathcal{A}, \mathcal{T}, \Omega, R, \gamma, \rho_0)$. $\mathcal{N} = \{1, \dots, N\}$ is a set of agents, $s \in \mathcal{S}$ denotes the state of the environment and ρ_0 is the distribution of the initial state. $\mathcal{A} = \prod_{i=1}^N A^i$ is the joint action space, $\mathbb{O} = \prod_{i=1}^N O^i$ is the set of joint observations. At time step t , each agent i receives an individual partial observation $o_t^i \in O^i$ given by the observation function $\mathcal{O} : (a_t, s_{t+1}) \mapsto P(o_{t+1}|a_t, s_{t+1})$ where a_t, s_{t+1} and o_{t+1} are the joint actions, states and joint observations respectively. Each agent i uses a stochastic policy $\pi^i(a_t^i|h_t^i, \omega_t^i)$ conditioned on its action-observation history $h_t^i = (o_0^i, a_0^i, \dots, o_{t-1}^i, a_{t-1}^i)$ and a random seed $\omega_t^i \in \Omega_t$ to choose an action $a_t^i \in A^i$. A belief state b_t is a probability distribution over states at time t , where $b_t \in \mathcal{B}$, and \mathcal{B} is the space of all probability distributions over the state space. Actions a_t drawn from joint policy $\pi(a_t|s_t, \omega_t)$ conditioned on state s_t and joint random seed $\omega_t = (\omega_1^1, \dots, \omega_t^N)$ change the state according to transition function $\mathcal{T} : (s_t, a_t^1, \dots, a_t^N) \mapsto P(s_{t+1}|s_t, a_t^1, \dots, a_t^N)$. All agents share the same reward $r_t = R(s_t, a_t^1, \dots, a_t^N)$ based on s_t and a_t . γ is the discount factor for future rewards. Agents try to maximize the expected total reward, $\mathcal{J}(\pi) = \mathbb{E}_{s_0, a_0, \dots} [\sum_{t=0}^{\infty} \gamma^t r_t]$, where $s_0 \sim \rho_0(s_0)$, $a_t \sim \pi(a_t|s_t, \omega_t)$.

Equilibrium Notions

We first define a *joint (potentially correlated) policy* as $\pi = \pi^1 \odot \pi^2 \dots \odot \pi^N$. We also denote $\pi^{-i} = \pi^1 \odot \dots \pi^{i-1} \odot \pi^{i+1} \odot \dots \odot \pi^N$ to be the joint policy excluding the i^{th} agent. A *product* policy is denoted as $\pi = \pi^1 \times \pi^2 \dots \times \pi^N$ if the distribution of drawing each seed ω_t^i for different agents is independent. We define the value function $V_{\pi^i, \pi^{-i}}^i(s)$ as the expected returns under state s that i^{th} agent will receive if all agents follow joint policy $\pi = (\pi^i, \pi^{-i})$:

$$V_{\pi^i, \pi^{-i}}^i(s) = \mathbb{E}_{a_{0:\infty}^i \sim \pi^i, a_{0:\infty}^{-i} \sim \pi^{-i}, s_{1:\infty} \sim \mathcal{T}} [\sum_{t=0}^{\infty} \gamma^t r_t | s_0 = s]. \quad (1)$$

A *strategy modification* for the i^{th} agent is a map $f^i : A^i \mapsto A^i$, which maps from the action set to itself. We can

define the resulting policy by applying the map on π^i as $f^i \diamond \pi^i$.

With the definition above, we can accordingly define the solution concepts.

Definition 1 (ϵ -approximate Nash Equilibrium). A **product** policy π_* is an ϵ -approximate Nash Equilibrium (NE) if for all $i \in \mathcal{N}$ and any $\epsilon \geq 0$:

$$V_{\pi_*, \pi_*^{-i}}^i(s) \geq \max_{\pi^i} V_{\pi^i, \pi_*^{-i}}^i(s) - \epsilon. \quad (2)$$

Definition 2 (ϵ -approximate Coarse Correlated Equilibrium). A **joint** policy π_* is an ϵ -approximate Coarse Correlated Equilibrium (CCE) if for all $i \in \mathcal{N}$ and any $\epsilon \geq 0$:

$$V_{\pi_*, \pi_*^{-i}}^i(s) \geq \max_{\pi^i} V_{\pi^i, \pi_*^{-i}}^i(s) - \epsilon. \quad (3)$$

The only difference between Definition 1 and Definition 2 is that an NE has to be a product policy while a CCE can be correlated.

Definition 3 (ϵ -approximate Correlated Equilibrium). A **joint** policy π_* is an ϵ -approximate Correlated Equilibrium (CE) if for all $i \in \mathcal{N}$ and any $\epsilon \geq 0$:

$$V_{\pi_*, \pi_*^{-i}}^i(s) \geq \max_{f^i} V_{(f^i \diamond \pi_*^i) \odot \pi_*^{-i}}^i(s) - \epsilon. \quad (4)$$

CCE forms a larger set of distributions than CE, and CE is richer than NE (i.e., $\text{NE} \subseteq \text{CE} \subseteq \text{CCE}$).

AgentMixer

In this work, we propose AgentMixer to achieve correlated policy factorization. The proposed method consists of two main components: *Policy Modifier* that models correlated joint fully observable policy and *Individual-Global-Consistency* that leverages the resulting joint policy for learning the individual policies while mitigating the *asymmetric information issue*.

Policy Modifier

To efficiently introduce correlation among agents, we propose *Policy Modifier*, a novel framework based entirely on multi-layer perceptrons (MLPs) (see the Appendix), which contains two types of MLP layers (Tolstikhin et al. 2021): *agent-mixing MLPs* and *channel-mixing MLPs*. The agent-mixing MLPs allow inter-agent communication; they operate on each channel of the feature independently. The channel-mixing MLPs allow intra-agent information fusion; they operate on each agent independently. These two types of layers are interleaved to enable the interaction among agents and the correlated representation of the joint policy. Specifically, agent- and channel-mixing can be written as follows:

$$\begin{aligned} \mathbf{H}_{\text{agent}} &= \mathbf{H}_{\text{input}} + \mathbf{W}_{\text{agent}}^{(2)} \sigma(\mathbf{W}_{\text{agent}}^{(1)} \text{LayerNorm}(\mathbf{H}_{\text{input}})), \\ \mathbf{H}_{\text{channel}} &= \mathbf{H}_{\text{agent}} + \sigma(\mathbf{W}_{\text{channel}}^{(1)} \text{LayerNorm}(\mathbf{H}_{\text{agent}})) \mathbf{W}_{\text{channel}}^{(2)}, \end{aligned} \quad (5)$$

where $\mathbf{H}_{\text{input}}$ is a concatenation of state features and individual policies features and \mathbf{W} denotes fully connected layers. The policy features are derived by compressing the policy

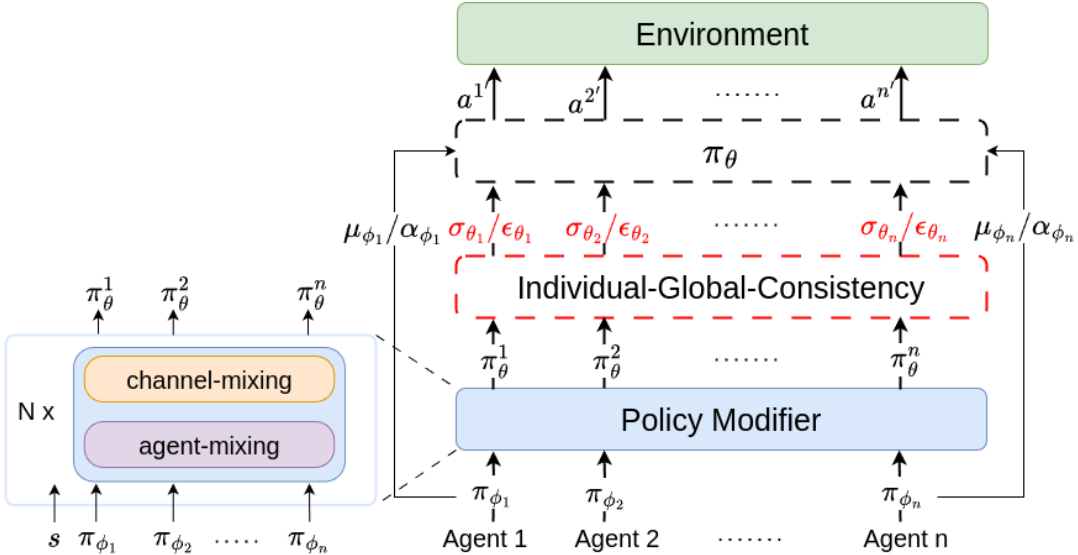


Figure 2: AgentMixer contains two components: 1) *Policy Modifier* takes the individual partially observable policies and state as inputs and produces correlated joint fully observable policy as outputs, and 2) *Individual-Global-Consistency* keeps the mode consistency among the joint policy and individual policies.

parameters through one MLP layer. In the continuous action space, the policy parameters are the mean and standard deviation, while in the discrete action space, the policy parameters are the logits. Then, the output of PM will be combined with individual policies to generate the correlated joint policy, denoted as $\text{PM}([\pi^i]_{i=1}^N) = ((f^1 \diamond \pi^1), \dots, (f^N \diamond \pi^N)) = (f^1 \diamond \pi^1) \odot (f^2 \diamond \pi^2) \dots \odot (f^N \diamond \pi^N)$, where f denotes a *strategy modification*. Consequently, PM maps the individual policies into a correlated joint policy by introducing dependencies among agents.

Individual Global Consistency

With the resulting correlated joint fully observable policy generated by PM, we can easily adopt different single-agent algorithms to get a (sub-)optimal correlated joint fully observable policy. To fulfill decentralized execution, we further ask a question:

Question 1: Can we just derive the decentralized partially observable policies by distilling the learned (sub-)optimal correlated joint fully observable policy?

In this section, we take several steps to provide a negative answer to the above research question. We begin by defining the joint policy and product policy as $\pi_\theta(a|s)$ and $\pi_\phi(a|b)$ respectively. Let the joint occupancy, $\rho^\pi(s, b)$, as the (improper) marginal state-belief distribution induced by a policy π : $\rho^\pi(s, b) = \sum_{t=0}^{\infty} \gamma^t P(s_t = s, b_t = b | \pi)$. Then, the marginal state distribution and marginal belief distribution induced by π are denoted as $\rho^\pi(s) = \int_b \rho^\pi(s, b) db$ and $\rho^\pi(b) = \int_s \rho^\pi(s, b) ds$ respectively. To distill the joint policy $\pi_\theta(a|s)$ into the product policy $\pi_\phi(a|b)$, previous work (Ye et al. 2022) leverage imitation learning, i.e., optimizing the asymmetric distillation objective:

$$\mathbb{E}_{\rho^{\pi_\beta}(s, b)} [D_{\text{KL}}(\pi_\theta(a|s) \| \pi_\phi(a|b))], \quad (6)$$

where $\pi_\beta(s, b) = \beta \pi_\theta(a|s) + (1 - \beta) \pi_\phi(a|b)$, π_β is a mixture of the joint policy $\pi_\theta(a|s)$, and the product policy $\pi_\phi(a|b)$. The coefficient β is annealed to zero during training. This avoids compounding error which grows with time horizon.

We then show that the optimal product policy defined by this objective can be expressed as posterior inference over state conditioned on the joint policy:

Definition 4 (Implicit product policy). For any correlated joint fully observable policy π_θ , product partially observable behavioral policy π_ψ , belief state b , and conditional occupancy ρ^{π_ψ} , we define $\hat{\pi}_\theta^\psi$ as the implicit product policy of π_θ under π_ψ as:

$$\hat{\pi}_\theta^\psi = \mathbb{E}_{\rho^{\pi_\psi}(s|b)} [\pi_\theta(a|s)]. \quad (7)$$

When $\pi_\psi = \hat{\pi}_\theta^\psi$, we refer to this product policy as the implicit product policy of π_θ , denoted as $\hat{\pi}_\theta$.

Implicit product policy is defined as a posterior inference procedure, marginalizing the conditional occupancy $\rho^{\pi_\psi}(s|b)$. Since the observations/belief may not contain information to distinguish two different latent states, the $\rho^{\pi_\psi}(s|b)$ is a stochastic distribution, and the implicit product policy is the average of the fully observable policy. Suppose a scenario where the agent learns to cross the ice while avoiding the pits in the middle of the ice. The fully observable policy which can observe the location of the pits will choose safer routes that avoid the pits, i.e., both sides of the ice. However, according to 7, the implicit policy that is not informed of the pit locations will take an average path of those safe routes, despite the danger of pits. The key insight is that directly imitating the fully observable policy will cause *asymmetric learning failure*. We show that the solution to the asymmetric distillation objective in 6 is equivalent to the implicit product policy 7 in the Appendix.

However, the implicit product policy requires marginalizing the conditional occupancy $\rho^\pi(s|b)$, which is intractable. Therefore, we can introduce a variational implicit product policy, π_η , as a proxy to the implicit product policy, which can be learned by minimizing the following objective:

$$\mathbb{E}_{\rho^{\pi_\psi}(s,b)} [D_{\text{KL}}(\pi_\theta(a|s) \parallel \pi_\eta(a|b))]. \quad (8)$$

Under sufficient expressiveness and exact updates assumptions, by setting $\pi_\psi = \pi_\eta$, updating 8 converges to the fixed point, i.e., the implicit product policy (see the Appendix).

We now reason about the *asymmetric learning failure*. To guarantee the optimal product partially observable policy, the divergence between the joint policy and product policy should be strictly zero, which we denote as *identifiability*:

Definition 5 (Identifiable policy pair). Given a correlated joint fully observable policy π_θ and a product partially observable policy π_ϕ , we define $\{\pi_\theta, \pi_\phi\}$ as an identifiable policy pair if and only if $\mathbb{E}_{\rho^{\pi_\phi}(s,b)} [D_{\text{KL}}(\pi_\theta(a|s) \parallel \pi_\phi(a|b))] = 0$.

Identifiable policy pairs require that the product partially observable policy can exactly recover the correlated joint fully observable policy. *Identifiability* then requires the optimal correlated joint fully observable policy and the corresponding implicit product policy to form an identifiable policy pair. Using *identifiability*, we can prove that given an optimal correlated joint fully observable policy, optimizing the asymmetric distillation objective is guaranteed to recover an optimal product partially observable policy:

Theorem 1 (Convergence of asymmetric distillation). *Given an optimal correlated joint fully observable policy π_{θ^*} being identifiability, the iteration defined by:*

$$\eta_{k+1} = \arg \min_{\eta} \mathbb{E}_{\rho^{\pi_{\eta_k}}(s,b)} [D_{\text{KL}}(\pi_{\theta^*}(a|s) \parallel \pi_\eta(a|b))] \quad (9)$$

converges to $\pi_{\eta^}(a|b)$ that defines an optimal product partially observable policy, as $k \rightarrow \infty$.*

Proof. See the Appendix for a detailed proof. \square

Theorem 1 shows that *identifiability* of the optimal joint policy defines a sufficient condition to guarantee the thorough distillation of the optimal joint fully observable policy into product partially observable policies. Unfortunately, the *identifiability* imposes a strong limitation on the applicability of asymmetric distillation. Hereby, we can conclude a negative answer to the **Question 1**. Therefore, we propose to modify the joint policy online by imposing a constraint on the mode between the joint policy and the decentralized policies to form an (approximately) identifiable policy pair. Furthermore, instead of naively applying distillation on the learned joint policy, we simultaneously learn the correlated joint fully observable policy and its product partially observable counterpart. We will show that the interleaving of the two learning processes moves the product partially observable policy closer to Correlated Equilibrium, i.e., the optimal product partially observable policy.

We now use the insight from Theorem 1 and the definition of *identifiability* to define *Individual-Global-Consistency*

(IGC), which keeps consistent modes between product partially observable policy and correlated joint fully observable policy.

Definition 6 (IGC). For a correlated joint fully observable policy $\pi_\theta(a|s)$, if there exists a product partially observable policy $\pi_\phi(a|b) = \pi_{\phi^1}(a|h^1) \times \pi_{\phi^2}(a|h^2) \cdots \times \pi_{\phi^N}(a|h^N)$, such that

$$\text{Mo}(\pi_\theta) = (\text{Mo}(\pi_{\phi^1}), \dots, \text{Mo}(\pi_{\phi^N})), \quad (10)$$

where $\text{Mo}(\cdot)$ denotes the mode of distribution. Then, we say that $\pi_\phi(a|b)$ satisfy IGC.

IGC enables the actions that occur most frequently in the joint policy and the product policy to be equivalent. Crucially, IGC minimizes the divergence between the two policies while allowing correlated exploration in the joint policy. One may find that IGC and IGM share some similarities. IGM ensures value-based individual optimal actions constitute the optimal joint action, while IGC maintains policy-based consistency with explicit consideration of partial observability. For a detailed clarification of the connection between IGC and IGM, please refer to the Appendix.

Implementation of IGC To preserve IGC, we adopt the method of disentanglement between exploration and exploitation to decompose the joint policy into two components: one for the mode (exploitation) and the other for the deviation (exploration). Then, IGC can be enforced through an equality constraint on the mode of joint policy and individual policies. Based on this disentanglement, agents are able to coordinate their exploration through the centralized policy. In practice, we divide the implementation of IGC into two categories: continuous action space and discrete action space.

Continuous Case: In this case, we assume the continuous action policy of agent i as a Gaussian distribution with mean μ_{ϕ^i} and standard deviation σ_{ϕ^i} : $\pi_{\phi^i}(a|h^i) = \mathcal{N}(\mu_{\phi^i}(h^i), \sigma_{\phi^i}^2(h^i))$. Since the mode of a Gaussian distribution is equal to the mean, we set the mean of joint policy as the collection of individual policies while the standard deviation is generated by PM: $\pi_\theta(a|s) = \mathcal{N}([\mu_{\phi^i}]_{i=1}^N, \sigma_\theta^2(s))$.

Discrete Case: In this case, we denote the discrete action policy of agent i as a categorical distribution parameterized by probabilities α_{ϕ^i} :

$$\pi_{\phi^i}(a|h^i) = \text{Cat}(\alpha_{\phi^i}(h^i)) = \text{softmax}(\alpha_{\phi^i}(h^i)), \quad (11)$$

where $\sum_{k=1}^K \alpha_{\phi^i}^k(h^i) = 1$. The mode of a categorical distribution is the category with the highest frequency. However, it is tricky to promote cooperative exploration while preserving the mode consistency. Fortunately, Gumbel-Softmax distribution (Jang, Gu, and Poole 2017) provides another perspective, where we explicitly disentangle exploration and mode. Specifically, we define the joint policy as:

$$\pi_\theta = \begin{pmatrix} \text{softmax}((\epsilon_\theta^1 + \log \alpha_{\phi^1})/\tau^1) \\ \vdots \\ \text{softmax}((\epsilon_\theta^N + \log \alpha_{\phi^N})/\tau^N) \end{pmatrix}, \quad (12)$$

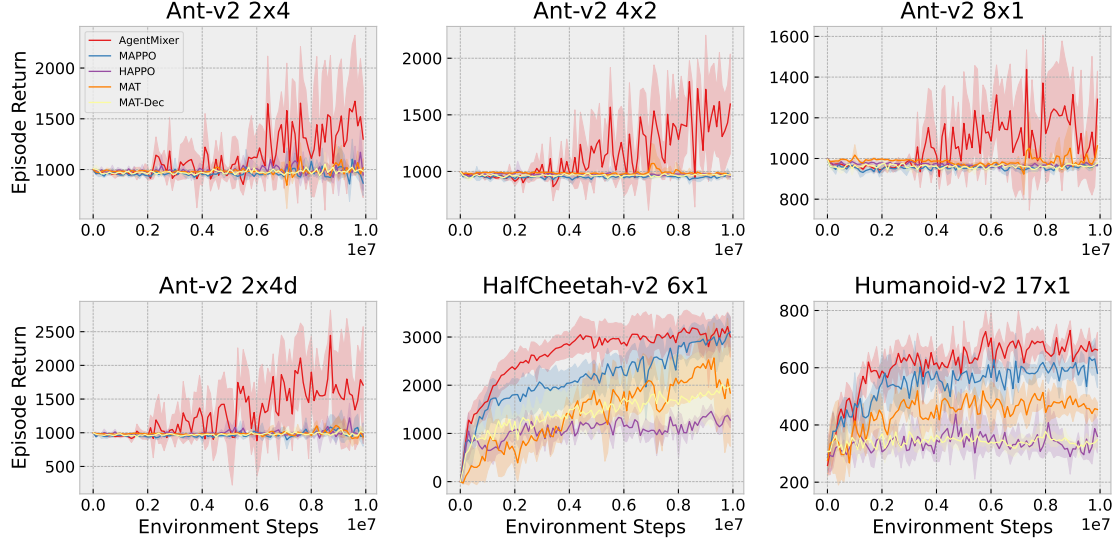


Figure 3: AgentMixer outperforms comparison methods on multiple Multi-Agent MuJoCo tasks. Please, see the statistical significance tests in the Appendix for further evidence. Partial observability in MA-MuJoCo is a critical challenge to most baselines.

where τ is a temperature hyperparameter and ϵ_θ is sampled using inverse transform sampling by generating $u_\theta \in (0, 1)$ with sigmoid function and computing $\epsilon_\theta = -\log(-\log(u_\theta))$. Note that when the temperature approaches 0, the joint policy degrades to the collection of individual policies.

Convergence of AgentMixer

Together with PM, we can treat the learning of the correlated joint fully observable policy as a single-agent RL problem where abundant single-agent methods with theoretical guarantees of convergence and performance exist:

$$\mathcal{J}(\pi_\theta) = \mathbb{E}_{s \sim \rho^{\pi_\theta}, a \sim \pi_\theta} \left[\sum_{t=0}^{\infty} \gamma^t r_t \right], \text{ subject to IGC, } (13)$$

where $\pi_\theta = \text{PM}([\pi_{\phi^i}]_{i=1}^N)$.

Theorem 2 (Convergence of AgentMixer). *The product partially observable policy generated by AgentMixer is a ϵ -CE.*

Proof. For proof see the Appendix. \square

With Theorem 2, we are ready to present the learning framework of AgentMixer, as illustrated in Figure 2, which consists of two main components: *Policy Modifier* and *Individual-Global-Consistency*. Specifically, PM acts as an observer who takes a holistic view and recommends that each agent follow her instructions. IGC then requires the agents to be obligated to follow the recommendations they receive. We provide the pseudo-code for AgentMixer in the Appendix. AgentMixer can benefit from a variety of strong single-agent algorithms, such as PPO (Schulman et al. 2017a) and SAC (Haarnoja et al. 2019). In this work,

our implementation of AgentMixer follows PPO (Schulman et al. 2017a).

Experiments

We compare our method AgentMixer with MAPPO (Yu et al. 2022), HAPPO (Kuba et al. 2021), MAVEN (Mahajan et al. 2019), ARMAPPO (Fu et al. 2022), MAT (Wen et al. 2022), and MAT with decentralized actor MAT-Dec. Note that our method and all comparison methods except MAT and MAT-Dec have access to only local information during evaluation. We evaluate on several continuous action space Multi-Agent MuJoCo (Peng et al. 2021) (*MA-MuJoCo*) benchmark tasks and discrete action space *SMAC-v2* (Ellis et al. 2022) benchmark tasks.¹ We include more experimental details and results on Climbing Matrix Game (Lauer and Riedmiller 2000) and Predator-Prey (Li et al. 2020) in the Appendix.

Continuous Actions Spaces: MA-MuJoCo

As in the full observation setting, previous methods have shown near-optimal performance in the *MA-MuJoCo* tasks (Kuba et al. 2021; Wen et al. 2022), we instead limit the set of observable elements for each agent to themselves, aiming to satisfy better the partial observability nature in MARL. We show the performance comparison against the baselines in Figure 3. We can see that AgentMixer enjoys superior performance over those baselines. The superiority of our method is highlighted especially in Ant-v2 tasks, where partial observability poses a critical challenge as the local observations of each agent (leg) of the ant are quite similar and make it hard to estimate the necessary state information for coordination. In these tasks, while other algorithms,

¹Code: github.com/LiZhYun/BackPropagationThroughAgents

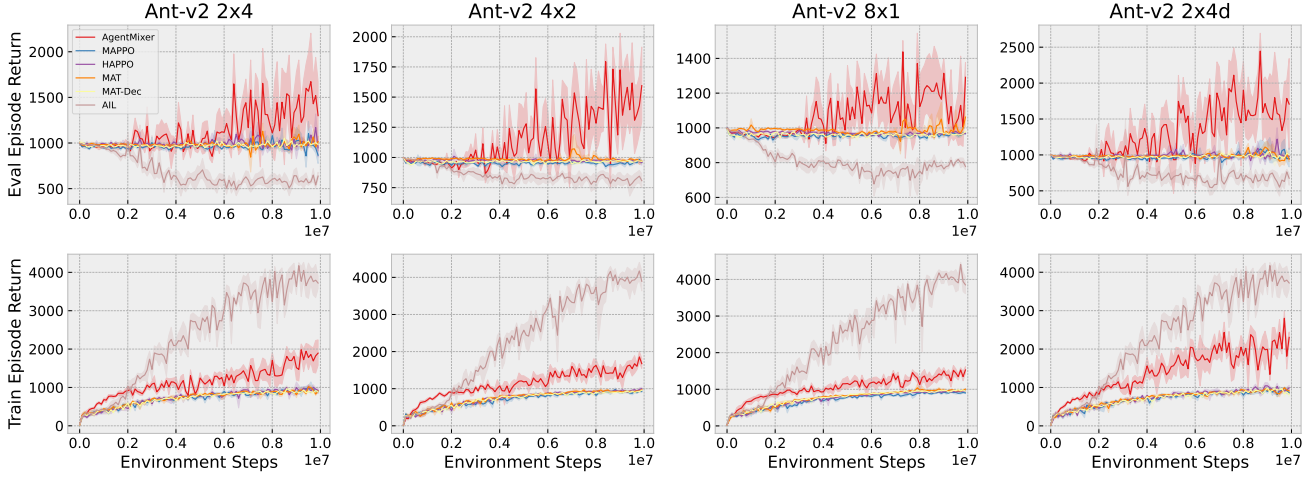


Figure 4: Ablations on Ant-v2. The large performance gap can be seen between training and testing on AIL, which is caused by *asymmetric learning failure*. Other baselines fail to learn any effective policies, while AgentMixer obtains superior performance.

| Map | MAPPO | HAPPO | MAT | MAT-Dec | MAVEN | ARMAPPO | Ours |
|---------------|-----------------------------|----------------------|-----------------------------|-----------------------------|-----------------------------|----------------------|-----------------------------|
| protoss 5v5 | 0.51 _{0.10} | 0.38 _{0.08} | 0.55 _{0.11} | 0.53 _{0.04} | 0.49 _{0.11} | 0.50 _{0.09} | 0.68 _{0.04} |
| terran 5v5 | 0.48 _{0.11} | 0.39 _{0.12} | 0.63 _{0.11} | 0.45 _{0.06} | 0.47 _{0.03} | 0.41 _{0.04} | 0.71 _{0.10} |
| zerg 5v5 | 0.48 _{0.05} | 0.39 _{0.05} | 0.48 _{0.10} | 0.51 _{0.10} | 0.46 _{0.08} | 0.44 _{0.06} | 0.66 _{0.03} |
| protoss 10v10 | 0.40 _{0.08} | 0.13 _{0.02} | 0.32 _{0.09} | 0.52 _{0.02} | 0.36 _{0.05} | 0.36 _{0.04} | 0.47 _{0.02} |
| terran 10v10 | 0.29 _{0.05} | 0.12 _{0.09} | 0.46 _{0.14} | 0.33 _{0.03} | 0.26 _{0.02} | 0.20 _{0.02} | 0.50 _{0.11} |
| zerg 10v10 | 0.38 _{0.12} | 0.29 _{0.07} | 0.52 _{0.09} | 0.36 _{0.05} | 0.46 _{0.05} | 0.36 _{0.06} | 0.52 _{0.06} |

Table 1: Median evaluate winning rate and standard deviation on six SMACv2 maps for different methods (steps=1e7). All values within 1 standard deviation of the maximum score rate are marked bold.

even the *centralized* MAT, fail to learn any meaningful joint policies, AgentMixer outperforms the baselines by a large margin. These results show that AgentMixer can effectively exploit asymmetric information to mitigate the challenges incurred by severe partial observability.

Discrete Action Spaces: SMAC-v2

Compared to the StarCraft Multi-Agent Challenge (SMAC), we instead evaluate our method on the more challenging SMAC-v2 benchmark which is designed with higher randomness. As shown in Table 1, AgentMixer outperforms other strong baselines in 5 out of 6 scenarios and achieves over 50% win rates in most maps, even over 70% in the terran 5v5 scenarios. Notably, in the 5v5 scenarios, we observe that AgentMixer improves win rates compared to the other six methods by a large margin, i.e. by 8% to 32%.

Ablation Results

To examine the effectiveness of AgentMixer in addressing *asymmetric learning failure*, we perform ablation experiments by adding an imitation learning baseline, asymmetric imitation learning (AIL) (Warrington et al. 2021), which uses PPO, conditioned on full state information, to supervise learning decentralized policies, conditioned on partial information. As shown in Figure 4, due to *asymmetric learning failure*, AIL performs poorly in evaluation, although

it achieves superior performance in training. In contrast, AgentMixer couples the learning of the centralized policy and decentralized policies such that partially observed policies can perform consistently with the fully observed policy.

Conclusion and Future Work

To achieve coordination among partially observable agents, this paper presents a novel framework named AgentMixer which enables *correlated policy factorization* and provably converges to ϵ -approximate Correlated Equilibrium. AgentMixer consists of two key components: 1) the *Policy Modifier* that takes all the initial decisions from individual agents and composes them into a correlated joint policy based on the full state information; 2) the *Individual-Global-Consistency* which mitigates the *asymmetric learning failure* by preserving the consistency between individual and joint policy. Surprisingly, IGC and IGM can be considered as parallel works of policy gradient-based and value-based methods respectively. We will study the transformation between IGC and IGM in future work. We extensively evaluate the proposed method in Multi-Agent MuJoCo, SMAC-v2, Matrix Game, and Predator-Prey. The experiments demonstrate that our method outperforms strong baselines in most tasks and achieves comparable performance in the rest.

Acknowledgments

This work was supported by the Research Council of Finland Flagship programme: Finnish Center for Artificial Intelligence FCAI.

References

Chen, L.; Guo, H.; Du, Y.; Fang, F.; Zhang, H.; Zhang, W.; and Yu, Y. 2022. Signal Instructed Coordination in Cooperative Multi-agent Reinforcement Learning. In Chen, J.; Lang, J.; Amato, C.; and Zhao, D., eds., *Distributed Artificial Intelligence*, 185–205. Cham: Springer International Publishing. ISBN 978-3-030-94662-3.

Drummond, G. B.; and Tom, B. D. 2011. Statistics, probability, significance, likelihood: words mean what we define them to mean. *British Journal of Pharmacology*, 164(6): 1573–1576.

Ellis, B.; Moalla, S.; Samvelyan, M.; Sun, M.; Mahajan, A.; Foerster, J. N.; and Whiteson, S. 2022. SMACv2: An Improved Benchmark for Cooperative Multi-Agent Reinforcement Learning. arXiv:2212.07489.

Feinberg, E.; and Shwartz, A. 2012. *Handbook of Markov Decision Processes: Methods and Applications*. International Series in Operations Research & Management Science. Springer US. ISBN 9781461508052.

Fu, W.; Yu, C.; Xu, Z.; Yang, J.; and Wu, Y. 2022. Revisiting Some Common Practices in Cooperative Multi-Agent Reinforcement Learning. In Chaudhuri, K.; Jegelka, S.; Song, L.; Szepesvari, C.; Niu, G.; and Sabato, S., eds., *Proceedings of the 39th International Conference on Machine Learning*, volume 162 of *Proceedings of Machine Learning Research*, 6863–6877. PMLR.

Greenwald, A.; and Hall, K. 2003. Correlated-Q Learning. In *Proceedings of the Twentieth International Conference on International Conference on Machine Learning*, ICML’03, 242–249. AAAI Press. ISBN 1577351894.

Gu, S.; Grudzien Kuba, J.; Chen, Y.; Du, Y.; Yang, L.; Knoll, A.; and Yang, Y. 2023. Safe multi-agent reinforcement learning for multi-robot control. *Artificial Intelligence*, 319: 103905.

Haarnoja, T.; Zhou, A.; Hartikainen, K.; Tucker, G.; Ha, S.; Tan, J.; Kumar, V.; Zhu, H.; Gupta, A.; Abbeel, P.; and Levine, S. 2019. Soft Actor-Critic Algorithms and Applications. arXiv:1812.05905.

Hong, Y.; Jin, Y.; and Tang, Y. 2022. Rethinking Individual Global Max in Cooperative Multi-Agent Reinforcement Learning. arXiv:2209.09640.

Hu, J.; and Wellman, M. P. 2003. Nash Q-Learning for General-Sum Stochastic Games. *J. Mach. Learn. Res.*, 4(null): 1039–1069.

Jang, E.; Gu, S.; and Poole, B. 2017. Categorical Reparameterization with Gumbel-Softmax. In *International Conference on Learning Representations*.

Kuba, J. G.; Chen, R.; Wen, M.; Wen, Y.; Sun, F.; Wang, J.; and Yang, Y. 2021. Trust Region Policy Optimisation in Multi-Agent Reinforcement Learning. *CoRR*, abs/2109.11251.

Lauer, M.; and Riedmiller, M. A. 2000. An Algorithm for Distributed Reinforcement Learning in Cooperative Multi-Agent Systems. In *Proceedings of the Seventeenth International Conference on Machine Learning*, ICML ’00, 535–542. San Francisco, CA, USA: Morgan Kaufmann Publishers Inc. ISBN 1558607072.

Li, C.; Liu, J.; Zhang, Y.; Wei, Y.; Niu, Y.; Yang, Y.; Liu, Y.; and Ouyang, W. 2023. ACE: Cooperative Multi-Agent Q-learning with Bidirectional Action-Dependency. *Proceedings of the AAAI Conference on Artificial Intelligence*, 37(7): 8536–8544.

Li, S.; Gupta, J. K.; Morales, P.; Allen, R.; and Kochenderfer, M. J. 2020. Deep implicit coordination graphs for multi-agent reinforcement learning. *arXiv preprint arXiv:2006.11438*.

Li, Z.; Wu, L.; Su, K.; Wu, W.; Jing, Y.; Wu, T.; Duan, W.; Yue, X.; Tong, X.; and Han, Y. 2024a. Coordination as inference in multi-agent reinforcement learning. *Neural Networks*, 172: 106101.

Li, Z.; Zhao, W.; Wu, L.; and Pajarinen, J. 2024b. Backpropagation Through Agents. *Proceedings of the AAAI Conference on Artificial Intelligence*, 38(12): 13718–13726.

Littman, M. L. 1994. Markov games as a framework for multi-agent reinforcement learning. In Cohen, W. W.; and Hirsh, H., eds., *Machine Learning Proceedings 1994*, 157–163. San Francisco (CA): Morgan Kaufmann. ISBN 978-1-55860-335-6.

Lowe, R.; Wu, Y.; Tamar, A.; Harb, J.; Pieter Abbeel, O.; and Mordatch, I. 2017. Multi-Agent Actor-Critic for Mixed Cooperative-Competitive Environments. In Guyon, I.; Luxburg, U. V.; Bengio, S.; Wallach, H.; Fergus, R.; Vishwanathan, S.; and Garnett, R., eds., *Advances in Neural Information Processing Systems*, volume 30. Curran Associates, Inc.

Ma, J.; and Wu, F. 2020. Feudal Multi-Agent Deep Reinforcement Learning for Traffic Signal Control. In Seghrouchni, A. E. F.; Sukthankar, G.; An, B.; and Yorke-Smith, N., eds., *Proceedings of the 19th International Conference on Autonomous Agents and Multiagent Systems, AAMAS ’20, Auckland, New Zealand, May 9-13, 2020*, 816–824. International Foundation for Autonomous Agents and Multiagent Systems.

Mahajan, A.; Rashid, T.; Samvelyan, M.; and Whiteson, S. 2019. MAVEN: Multi-Agent Variational Exploration. In Wallach, H.; Larochelle, H.; Beygelzimer, A.; d’Alché-Buc, F.; Fox, E.; and Garnett, R., eds., *Advances in Neural Information Processing Systems*, volume 32. Curran Associates, Inc.

Maschler, M.; Zamir, S.; and Solan, E. 2013. *Game Theory*. Cambridge University Press. ISBN 9781107005488.

Oliehoek, F. A.; and Amato, C. 2016. *A Concise Introduction to Decentralized POMDPs*. Springer Publishing Company, Incorporated, 1st edition. ISBN 3319289276.

Pajarinen, J.; Hottinen, A.; and Peltonen, J. 2014. Optimizing Spatial and Temporal Reuse in Wireless Networks by

Decentralized Partially Observable Markov Decision Processes. *IEEE Transactions on Mobile Computing*, 13(4): 866–879.

Peng, B.; Rashid, T.; Schroeder de Witt, C.; Kamienny, P.-A.; Torr, P.; Boehmer, W.; and Whiteson, S. 2021. FAC-MAC: Factored Multi-Agent Centralised Policy Gradients. In Ranzato, M.; Beygelzimer, A.; Dauphin, Y.; Liang, P.; and Vaughan, J. W., eds., *Advances in Neural Information Processing Systems*, volume 34, 12208–12221. Curran Associates, Inc.

Phan, T.; Ritz, F.; Altmann, P.; Zorn, M.; Nüßlein, J.; Kölle, M.; Gabor, T.; and Linnhoff-Popien, C. 2023. Attention-Based Recurrence for Multi-Agent Reinforcement Learning under Stochastic Partial Observability. In *Proceedings of the 40th International Conference on Machine Learning*, ICML’23. JMLR.org.

Rashid, T.; Samvelyan, M.; De Witt, C. S.; Farquhar, G.; Foerster, J.; and Whiteson, S. 2020. Monotonic Value Function Factorisation for Deep Multi-Agent Reinforcement Learning. *J. Mach. Learn. Res.*, 21(1).

Schroeder de Witt, C.; Foerster, J.; Farquhar, G.; Torr, P.; Boehmer, W.; and Whiteson, S. 2019. Multi-Agent Common Knowledge Reinforcement Learning. In Wallach, H.; Larochelle, H.; Beygelzimer, A.; d’Alché-Buc, F.; Fox, E.; and Garnett, R., eds., *Advances in Neural Information Processing Systems*, volume 32. Curran Associates, Inc.

Schulman, J.; Levine, S.; Abbeel, P.; Jordan, M.; and Moritz, P. 2015. Trust Region Policy Optimization. In Bach, F.; and Blei, D., eds., *Proceedings of the 32nd International Conference on Machine Learning*, volume 37 of *Proceedings of Machine Learning Research*, 1889–1897. Lille, France: PMLR.

Schulman, J.; Wolski, F.; Dhariwal, P.; Radford, A.; and Klimov, O. 2017a. Proximal Policy Optimization Algorithms. *arXiv*:1707.06347.

Schulman, J.; Wolski, F.; Dhariwal, P.; Radford, A.; and Klimov, O. 2017b. Proximal Policy Optimization Algorithms. *CoRR*, abs/1707.06347.

Shalev-Shwartz, S.; Shammah, S.; and Shashua, A. 2016. Safe, Multi-Agent, Reinforcement Learning for Autonomous Driving. *CoRR*, abs/1610.03295.

Sheng, J.; Li, W.; Jin, B.; Zha, H.; Wang, J.; and Wang, X. 2023. Negotiated Reasoning: On Provably Addressing Relative Over-Generalization. *arXiv*:2306.05353.

Son, K.; Kim, D.; Kang, W. J.; Hostallero, D. E.; and Yi, Y. 2019. QTRAN: Learning to Factorize with Transformation for Cooperative Multi-Agent Reinforcement Learning. In Chaudhuri, K.; and Salakhutdinov, R., eds., *Proceedings of the 36th International Conference on Machine Learning*, volume 97 of *Proceedings of Machine Learning Research*, 5887–5896. PMLR.

Sunehag, P.; Lever, G.; Gruslys, A.; Czarnecki, W. M.; Zambaldi, V.; Jaderberg, M.; Lanctot, M.; Sonnerat, N.; Leibo, J. Z.; Tuyls, K.; and Graepel, T. 2017. Value-Decomposition Networks For Cooperative Multi-Agent Learning. *arXiv*:1706.05296.

Tolstikhin, I. O.; Houlsby, N.; Kolesnikov, A.; Beyer, L.; Zhai, X.; Unterthiner, T.; Yung, J.; Steiner, A.; Keysers, D.; Uszkoreit, J.; Lucic, M.; and Dosovitskiy, A. 2021. MLP-Mixer: An all-MLP Architecture for Vision. In Ranzato, M.; Beygelzimer, A.; Dauphin, Y.; Liang, P.; and Vaughan, J. W., eds., *Advances in Neural Information Processing Systems*, volume 34, 24261–24272. Curran Associates, Inc.

Vaswani, A.; Shazeer, N.; Parmar, N.; Uszkoreit, J.; Jones, L.; Gomez, A. N.; Kaiser, L. u.; and Polosukhin, I. 2017. Attention is All you Need. In Guyon, I.; Luxburg, U. V.; Bengio, S.; Wallach, H.; Fergus, R.; Vishwanathan, S.; and Garnett, R., eds., *Advances in Neural Information Processing Systems*, volume 30. Curran Associates, Inc.

Walsman, A.; Zhang, M.; Choudhury, S.; Fox, D.; and Farhadi, A. 2023. Impossibly Good Experts and How to Follow Them. In *The Eleventh International Conference on Learning Representations*.

Wang, J.; Ren, Z.; Liu, T.; Yu, Y.; and Zhang, C. 2021a. {QPLEX}: Duplex Dueling Multi-Agent Q-Learning. In *International Conference on Learning Representations*.

Wang, J.; Ye, D.; and Lu, Z. 2023. More Centralized Training, Still Decentralized Execution: Multi-Agent Conditional Policy Factorization. In *The Eleventh International Conference on Learning Representations*.

Wang, Y.; Han, B.; Wang, T.; Dong, H.; and Zhang, C. 2021b. {DOP}: Off-Policy Multi-Agent Decomposed Policy Gradients. In *International Conference on Learning Representations*.

Warrington, A.; Lavington, J. W.; Scibior, A.; Schmidt, M.; and Wood, F. 2021. Robust Asymmetric Learning in POMDPs. In Meila, M.; and Zhang, T., eds., *Proceedings of the 38th International Conference on Machine Learning*, volume 139 of *Proceedings of Machine Learning Research*, 11013–11023. PMLR.

Wen, M.; Kuba, J.; Lin, R.; Zhang, W.; Wen, Y.; Wang, J.; and Yang, Y. 2022. Multi-Agent Reinforcement Learning is a Sequence Modeling Problem. In Koyejo, S.; Mohamed, S.; Agarwal, A.; Belgrave, D.; Cho, K.; and Oh, A., eds., *Advances in Neural Information Processing Systems*, volume 35, 16509–16521. Curran Associates, Inc.

Ye, J.; Li, C.; Wang, J.; and Zhang, C. 2022. Towards global optimality in cooperative marl with sequential transformation. *arXiv preprint arXiv:2207.11143*.

Yu, C.; Velu, A.; Vinitsky, E.; Gao, J.; Wang, Y.; Bayen, A.; and Wu, Y. 2022. The Surprising Effectiveness of PPO in Cooperative Multi-Agent Games. In Koyejo, S.; Mohamed, S.; Agarwal, A.; Belgrave, D.; Cho, K.; and Oh, A., eds., *Advances in Neural Information Processing Systems*, volume 35, 24611–24624. Curran Associates, Inc.

Zhang, T.; Li, Y.; Wang, C.; Xie, G.; and Lu, Z. 2021. FOP: Factorizing Optimal Joint Policy of Maximum-Entropy Multi-Agent Reinforcement Learning. In Meila, M.; and Zhang, T., eds., *Proceedings of the 38th International Conference on Machine Learning*, volume 139 of *Proceedings of Machine Learning Research*, 12491–12500. PMLR.

Detail structure of Policy Modifier

Figure 5 depicts the macro-structure of *Policy Modifier*. It accepts the state and policies of agents as input. Specifically, *Policy Modifier* two MLP blocks. The first one is the *agent-mixing MLPs*: it acts on columns of input. The second one is the *channel-mixing MLP*: it acts on rows of the output of *agent-mixing MLPs*.

Additional Proofs

Proof of Lemma 1

Lemma 1 (Asymmetric distillation solution). *For any correlated joint fully observable policy π_θ and fixed product partially observable behavioral policy π_ψ , the implicit product policy $\hat{\pi}_\theta^\psi$, defined in Definition 4, minimizes the asymmetric distillation objective:*

$$\hat{\pi}_\theta^\psi = \arg \min_{\pi} \mathbb{E}_{\rho^{\pi_\psi}(s, b)} [D_{\text{KL}}(\pi_\theta(a|s) \parallel \pi(a|b))]. \quad (14)$$

Proof. Expanding the right-hand side:

$$\begin{aligned} & \arg \min_{\pi} \mathbb{E}_{\rho^{\pi_\psi}(s, b)} [D_{\text{KL}}(\pi_\theta(a|s) \parallel \pi(a|b))] \\ &= \arg \min_{\pi} \mathbb{E}_{\rho^{\pi_\psi}(b)} \left[\int_s \int_a \pi_\theta(a|s) \log \left(\frac{\pi_\theta(a|s)}{\pi(a|b)} \right) da \rho^{\pi_\psi}(s|b) ds \right], \\ &= \arg \min_{\pi} \mathbb{E}_{\rho^{\pi_\psi}(b)} \left[\int_s \mathcal{H}(\pi_\theta(\cdot|s)) \rho^{\pi_\psi}(s|b) ds \right] - \\ & \quad \mathbb{E}_{\rho^{\pi_\psi}(b)} \left[\int_s \int_a \pi_\theta(a|s) \log(\pi(a|b)) da \rho^{\pi_\psi}(s|b) ds \right], \end{aligned}$$

where $\mathcal{H}(\cdot)$ is the entropy function,

$$\begin{aligned} &= \arg \min_{\pi} \text{const} - \mathbb{E}_{\rho^{\pi_\psi}(b)} \left[\int_a \hat{\pi}_\theta^\psi(a|b) \log(\pi(a|b)) da \right], \\ &\text{note that we are free to set the const,} \\ &\text{so long as it remains independent of } \pi, \\ &= \arg \min_{\pi} \mathbb{E}_{\rho^{\pi_\psi}(b)} \left[\int_a \hat{\pi}_\theta^\psi(a|b) \log(\hat{\pi}_\theta^\psi(a|b)) da - \right. \\ & \quad \left. \int_a \hat{\pi}_\theta^\psi(a|b) \log(\pi(a|b)) da \right], \\ &= \arg \min_{\pi} \mathbb{E}_{\rho^{\pi_\psi}(b)} \left[D_{\text{KL}}(\hat{\pi}_\theta^\psi(a|b) \parallel \pi(a|b)) \right]. \end{aligned} \quad (15)$$

Hence we conclude the proof. \square

Proof of Convergence of Iterative Variational Approximation

We first introduce an assumption which simply states that the variational family is sufficiently expressive such that the implicit product policy can be recovered, and the implicit product policy is sufficiently expressive such that the optimal product partially observable policy can actually be found.

Assumption 1 (Sufficiency of Variational Representations). We assume that for any product behavioral policy, π_ψ , the variational family is sufficiently expressive such that any implicit product policy, $\hat{\pi}_\theta$, can be exactly recovered under

the occupancy induced by the product behavioral policy. We also assume that there is an implicit product policy, $\hat{\pi}_\theta$, such that an optimal product partially observable policy can be represented, and thus there is a variational implicit product policy that can represent the optimal product partially observable policy under $\rho^{\pi_\psi}(b)$.

We then introduce the lemma which shows that the solution to an iterative procedure actually converges to the solution of a single equivalent “static” optimization problem. This lemma allows us to solve the challenging optimization using a simple iterative procedure.

Lemma 2 (Convergence of Iterative Variational Approximation). *Given the implicit product policy $\hat{\pi}_\theta$ and the corresponding variational approximation to $\hat{\pi}_\theta$, π_η , then under Assumption 1, the iterative procedure:*

$$\eta_{k+1} = \arg \min_{\eta} \mathbb{E}_{\rho^{\pi_{\eta_k}}(b)} [D_{\text{KL}}(\hat{\pi}_\theta(a|b) \parallel \pi_\eta(a|b))], \quad (16)$$

converges to the solution to the optimization problem with $k \rightarrow \infty$:

$$\eta^* = \arg \min_{\eta} \mathbb{E}_{\rho^{\pi_\eta}(b)} [D_{\text{KL}}(\hat{\pi}_\theta(a|b) \parallel \pi_\eta(a|b))]. \quad (17)$$

Proof. We begin by expressing the total variation between $\rho^{\pi_{\eta^*}}(b)$ and $\rho^{\pi_{\eta^k}}(b)$ at the k^{th} iteration:

$$\begin{aligned} D_{\text{TV}}(\rho^{\pi_{\eta^*}}(b) \parallel \rho^{\pi_{\eta^k}}(b)) &= \\ & \sup_b |\sum_{t=0}^{\infty} \gamma^t P(b_t = b | \pi_{\eta^*}) - \sum_{t=0}^{\infty} \gamma^t P(b_t = b | \pi_{\eta^k})|, \\ &= \sup_b |\sum_{t=0}^k \gamma^t P(b_t = b | \pi_{\eta^*}) + \sum_{t=k+1}^{\infty} \gamma^t P(b_t = b | \pi_{\eta^*}) \\ & \quad - \sum_{t=0}^k \gamma^t P(b_t = b | \pi_{\eta^k}) - \sum_{t=k+1}^{\infty} \gamma^t P(b_t = b | \pi_{\eta^k})|. \end{aligned} \quad (18)$$

We can then note that at the k^{th} iteration, the marginal belief distributions induced by π_{η^*} and π_{η^k} over the first k iteration must be identical as the underlying dynamics are the same at the initial state and belief state and we have exactly minimized the $D_{\text{KL}}(\pi_{\eta^*} \parallel \pi_{\eta^k})$. With the assumption that the maximum variation between the densities is bounded by C , we have:

$$\begin{aligned} & \sup_b |\sum_{t=0}^k \gamma^t P(b_t = b | \pi_{\eta^*}) + \sum_{t=k+1}^{\infty} \gamma^t P(b_t = b | \pi_{\eta^*}) \\ & \quad - \sum_{t=0}^k \gamma^t P(b_t = b | \pi_{\eta^k}) - \sum_{t=k+1}^{\infty} \gamma^t P(b_t = b | \pi_{\eta^k})|, \\ &= \sup_b |\sum_{t=k+1}^{\infty} \gamma^t (P(b_t = b | \pi_{\eta^*}) - P(b_t = b | \pi_{\eta^k}))|, \\ &\leq \sup_b |\sum_{t=k+1}^{\infty} \gamma^t C|, \\ &= C \left(\frac{1}{1-\gamma} - \frac{1-\gamma^{k+1}}{1-\gamma} \right), \\ &= C \frac{\gamma^{k+1}}{1-\gamma} = O(\gamma^k). \end{aligned} \quad (19)$$

Hence, as $\gamma \in [0, 1)$, the total variation between π_{η^*} and π_{η^k} converges to zero as $k \rightarrow \infty$. With this result and the expressiveness assumption, we complete the proof. \square

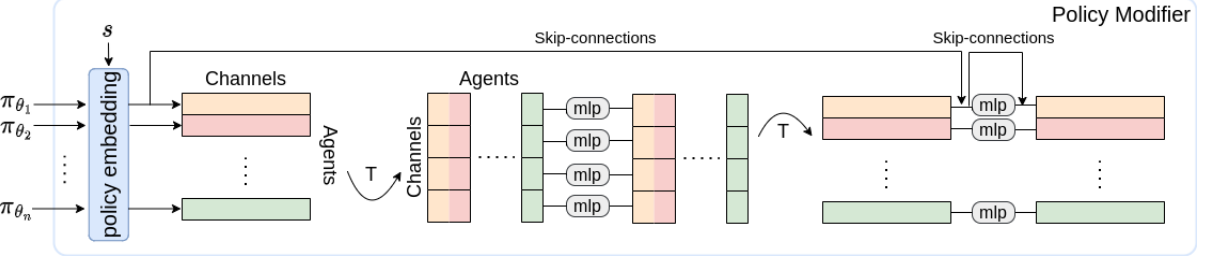


Figure 5: Policy Modifier consists of policy embedding layer, agent-mixing MLP and channel-mixing MLP.

Similar to the proof of Lemma 2, we can derive the following result:

$$\begin{aligned} \arg \min_{\eta} \mathbb{E}_{\rho^{\pi_{\psi}(b)}} [D_{\text{KL}} (\hat{\pi}_{\theta}(a|b) \| \pi_{\eta}(a|b))] = \\ \arg \min_{\eta} \mathbb{E}_{\rho^{\hat{\pi}_{\theta}(b)}} [D_{\text{KL}} (\hat{\pi}_{\theta}(a|b) \| \pi_{\eta}(a|b))]. \end{aligned} \quad (20)$$

This result allows us to exchange the distribution under which we take expectations.

Proof of Theorem 1

With Assumption 1, Lemma 2, and the identifiability condition, we are ready to verify the convergence of asymmetric distillation.

Theorem 1 (Convergence of asymmetric distillation). *Given an optimal correlated joint fully observable policy π_{θ^*} being identifiability, the iteration defined by:*

$$\eta_{k+1} = \arg \min_{\eta} \mathbb{E}_{\rho^{\pi_{\eta_k}(s, b)}} [D_{\text{KL}} (\pi_{\theta^*}(a|s) \| \pi_{\eta}(a|b))] \quad (9)$$

converges to $\pi_{\eta^*}(a|b)$ that defines an optimal product partially observable policy, as $k \rightarrow \infty$.

Proof. We begin by considering the limiting behavior as $k \rightarrow \infty$:

$$\begin{aligned} \eta^* &= \lim_{k \rightarrow \infty} \arg \min_{\eta} \mathbb{E}_{\rho^{\pi_{\eta_k}(s, b)}} [D_{\text{KL}} (\pi_{\theta^*}(a|s) \| \pi_{\eta}(a|b))], \\ &= \lim_{k \rightarrow \infty} \arg \min_{\eta} \mathbb{E}_{\rho^{\pi_{\eta_k}(b)}} [D_{\text{KL}} (\hat{\pi}_{\theta^*}(a|b) \| \pi_{\eta}(a|b))], \\ &= \arg \min_{\eta} \mathbb{E}_{\rho^{\pi_{\eta}(b)}} [D_{\text{KL}} (\hat{\pi}_{\theta^*}(a|b) \| \pi_{\eta}(a|b))], \\ &= \arg \min_{\eta} \mathbb{E}_{\rho^{\hat{\pi}_{\theta^*}(b)}} [D_{\text{KL}} (\pi_{\theta^*}(a|b) \| \pi_{\eta}(a|b))], \\ &= \arg \min_{\eta} \mathbb{E}_{\rho^{\pi_{\phi^*}(b)}} [D_{\text{KL}} (\pi_{\phi^*}(a|b) \| \pi_{\eta}(a|b))]. \end{aligned} \quad (21)$$

Finally, under Assumption 1, the expected KL divergence can be exactly zero, which completes the proof. \square

Proof of Theorem 2

Theorem 2 (Convergence of AgentMixer). *The product partially observable policy generated by AgentMixer is a ϵ -CE.*

Proof. Since PM modifies the decentralized policies and generates the correlated joint policy, i.e., $\pi_{\theta} = ((f_{\theta}^1 \diamond \dots \diamond f_{\theta}^N))$,

$\pi_{\phi^1}, \dots, (f_{\theta}^N \diamond \pi_{\phi^N}))$, the RL procedure mentioned in 13 can be regarded as a single-agent RL problem. By leveraging Theorem 1 in TRPO (Schulman et al. 2015), we can conclude that a sequence $(\pi_{\theta_k})_{k=1}^{\infty}$ of joint policies updated by 13 has the monotonic improvement property, i.e., $\mathcal{J}(\pi_{\theta_{k+1}}) \geq \mathcal{J}(\pi_{\theta_k})$. According to Bolzano-Weierstrass Theorem, the sequence of policies $(\pi_{\theta_k})_{k=1}^{\infty}$ exists at least one sub-optimal point π_{θ^*} . Let $\pi_{\bar{\theta}}$ be the optimal joint policy and $\epsilon = V_{\pi_{\bar{\theta}}}(s) - V_{\pi_{\theta^*}}(s) \geq 0$. Given the value function defined in 1, we have:

$$V_{\pi_{\theta^*}}(s) + \epsilon \geq V_{\pi_{\theta}}(s), \forall \pi_{\theta}. \quad (22)$$

Since optimizing π_{θ} is actually optimizing f_{θ} , then we can obtain:

$$V_{((f_{\theta^*}^1 \diamond \pi_{\phi^1}), \dots, (f_{\theta^*}^N \diamond \pi_{\phi^N}))}(s) + \epsilon \geq \max_{f_{\theta}} V_{((f_{\theta}^1 \diamond \pi_{\phi^1}), \dots, (f_{\theta}^N \diamond \pi_{\phi^N}))}(s). \quad (23)$$

Applying IGC, which keeps the mode consistency between joint policy and product policy, yields:

$$((f_{\theta^*}^1 \diamond \pi_{\phi^1}), \dots, (f_{\theta^*}^N \diamond \pi_{\phi^N})) = (\pi_{\phi^1}, \dots, \pi_{\phi^N}). \quad (24)$$

Finally, by plugging 24 into 23:

$$V_{(\pi_{\phi^1}, \dots, \pi_{\phi^N})}(s) \geq \max_{f_{\theta}} V_{((f_{\theta}^1 \diamond \pi_{\phi^1}), \dots, (f_{\theta}^N \diamond \pi_{\phi^N}))}(s) - \epsilon. \quad (25)$$

which is exactly the ϵ -CE defined in Definition 3. \square

Relationship Between IGC and IGM

IGM affirms the optimal action consistency between the global and local policies, which can be represented as follows (Hong, Jin, and Tang 2022):

$$\begin{cases} \arg \max_a Q_{\text{tot}}(s, a) = \begin{pmatrix} \arg \max_{a^1} Q_1(s, a^1) \\ \vdots \\ \arg \max_{a^N} Q_N(s, a^N) \end{pmatrix} \\ \begin{pmatrix} \arg \max_{a^1} Q_1(s, a^1) \\ \vdots \\ \arg \max_{a^N} Q_N(s, a^N) \end{pmatrix} = \begin{pmatrix} \arg \max_{a^1} q_1(h^1, a^1) \\ \vdots \\ \arg \max_{a^N} q_N(h^N, a^N) \end{pmatrix} \end{cases}. \quad (26)$$

where Q_{tot} is the joint action value function based on the global state, Q_i and q_i are the local action value functions based on the global state and the local history respectively.

IGC and IGM share a lot of similarities as they both pursue the consistency of global and local policy. Both of them

attempt to convert state-dependent policy into observation-dependent policy.

On the other hand, one of the differences is that IGM is imposed on joint action value function and local action value, while IGC explicitly maintains mode consistency between joint policy and individual policies. Moreover, Eq. 26 indicates that IGM directly maps state-based action value into observation-based action value without considering the issue of mismatch between global state and local observation. We can infer the same result as in previous work (Phan et al. 2023) based on Definition 4, that is, the observation-based action value is the average of the state-based action value under the conditional occupancy. On the contrary, IGC modifies the joint policy according to the individual policies, such that the modified joint policy and corresponding implicit product policy pair form an identifiable policy pair under partial observation. Consequently, this modification ensures that the joint policy provides consistent guidance.

Pseudo-code for AgentMixer

The pseudo-code of our method is shown in Algorithm .

Algorithm 1: AgentMixer

```

INITIALIZE Decentralized partially observable policies
 $\{\pi_{\phi^1}, \dots, \pi_{\phi^N}\}$ , a single agent algorithm A.
//Construct the joint policy:
 $\pi_{\theta} = \text{PM}([\pi_{\phi^i}]_{i=1}^N)$ , subjected to IGC.
Run A on  $\pi_{\theta}$ .
RETURN  $\{\pi_{\phi^1}, \dots, \pi_{\phi^N}\}$ .

```

Baselines and More Experiments

We compare our method with the baselines below including both algorithms with state-of-the-art performance and methods designed specifically to tackle the coordination problems.

MAPPO (Yu et al. 2022) applies PPO (Schulman et al. 2017b) to multi-agent settings and utilizes CTDE to learn critics based on the global state in order to stabilize the policy gradient estimation. Although with simple techniques, MAPPO has achieved tremendous empirical success in various multi-agent domains and can be a strong baseline for our method.

HAPPO (Kuba et al. 2021) performs sequential policy updates by utilizing other agents' newest policy under the CTDE framework and provably obtains the monotonic policy improvement guarantee as in single-agent PPO.

MAT (oracle) & MAT-Dec (Wen et al. 2022) model the multi-agent decision process as a sequence-to-sequence generation problem with powerful transformer architecture (Vaswani et al. 2017). Note that MAT is not a comparison method, but we have it as some performance upper bound in the experiments. *MAT-Dec* is the decentralized version of *MAT* which relaxes the restriction of using other agents' actions but remains taking the full observations from other agents. Therefore, we remind that *MAT* & *MAT-Dec*

uses full state information in experiments while our method and other baselines are limited by partial observation.

MAVEN (Mahajan et al. 2019) is proposed to improve the exploration of QMIX by introducing a latent space for hierarchical control. Compared to QMIX, MAVEN takes further advantage of CTDE through a *committed exploration* strategy.

ARMAPPO (Fu et al. 2022) extends PPO into multi-agent settings and explicitly introduces auto-regressive dependency among agents.

AIL (Warrington et al. 2021) naively distills partially observable agents' policies from the fully observable centralized policy. Although showing significant training performance, it suffers from the *asymmetric learning failure* problem and fails to perform well during execution with partial observation.

We summarize the different CTDE settings in Table 2. Note that although MAT and MAT-Dec sometimes show better performance than other methods, they take the full state information even during execution.

More Experiments on MA-MuJoCo

Inspired by mujoco tasks in the single-agent RL realm, *MA-MuJoCo* splits the joints of robots into different agents to enable decentralized control for MARL research. *MA-MuJoCo* allows different observation settings by changing the parameter of *obsk* which controls the number of neighbor joints each agent can observe.

We show the experiment results on more *MA-MuJoCo* tasks in Figure 6. Extended ablation study results are shown in Figure 7.

More Experiments on SMAC-v2

The original StarCraft Multi-Agent Challenge (*SMAC*) has been shown to be not difficult enough, as an open-loop policy conditioned only on the timestep can achieve non-trivial win rates for many scenarios. To address these shortcomings, a new benchmark, SMACv2 was proposed to address *SMAC*'s lack of stochasticity.

We compare a baseline, MAPPO_FULL, conditioned on full state information during evaluation. The results in Fig. 10 show that partially observable policies achieve similar performance as fully observable policies. This demonstrates that global information is not important for learning in the SMACv2 domain.

More Experiments on Climbing Matrix Game

The climbing matrix game (Lauer and Riedmiller 2000) has the payoff shown in the left of Figure 11. In this task, there are two agents to select the column and row index of the matrix respectively. The goal is to select the maximal element in the matrix. Although stateless and with simple action space, *Climbing* is difficult to solve via independent learning, as the agents need to coordinate among two optimal joint actions. The right of Figure 11 shows that the almost compared baselines converge to a local optimum while only AgentMixer and MAT successfully learn the optimal policy. This is reasonable, as in MAPPO, HAPPO, and MAT-Dec,

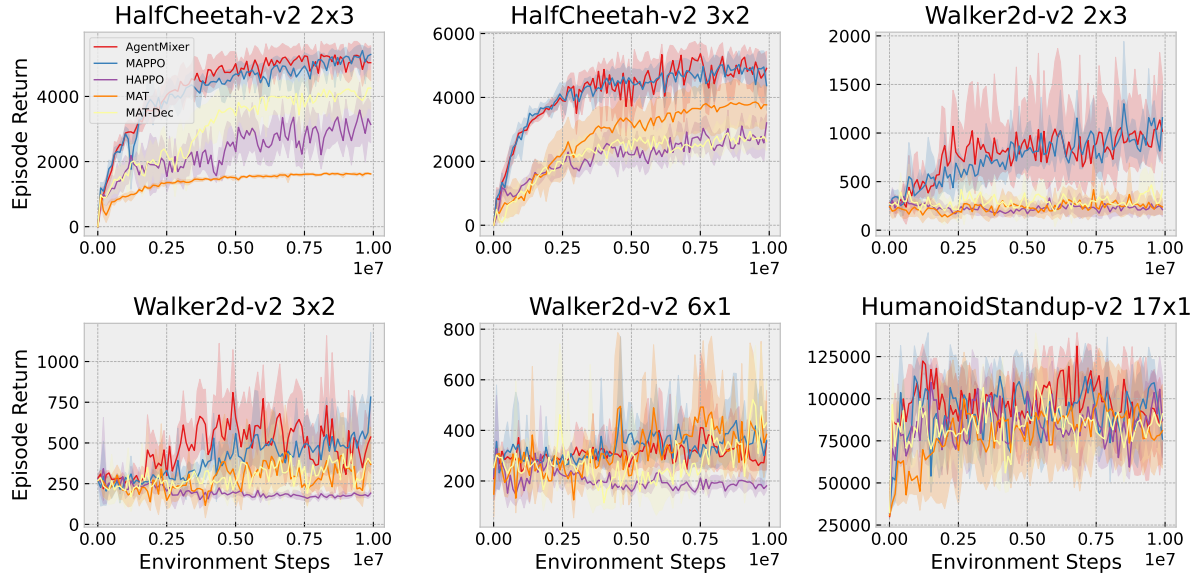


Figure 6: Performance comparison on multiple Multi-Agent MuJoCo tasks.

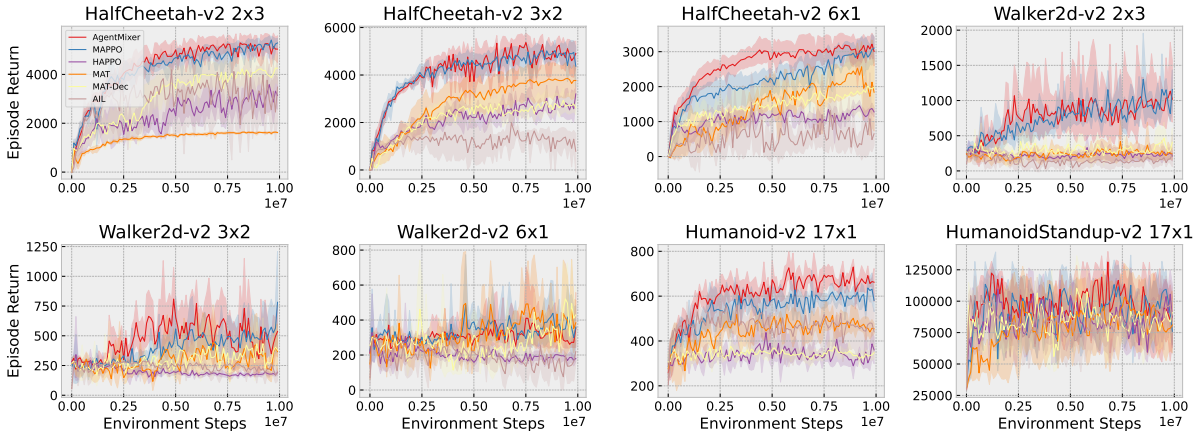


Figure 7: Ablations on multiple Multi-Agent MuJoCo tasks.

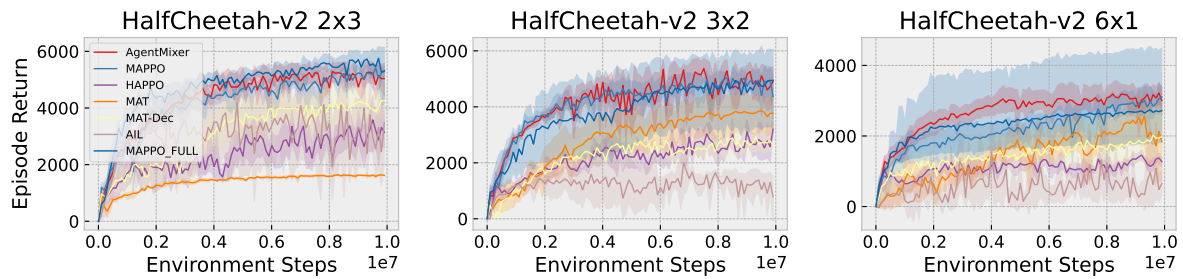


Figure 8: Ablations on multiple Multi-Agent MuJoCo tasks.

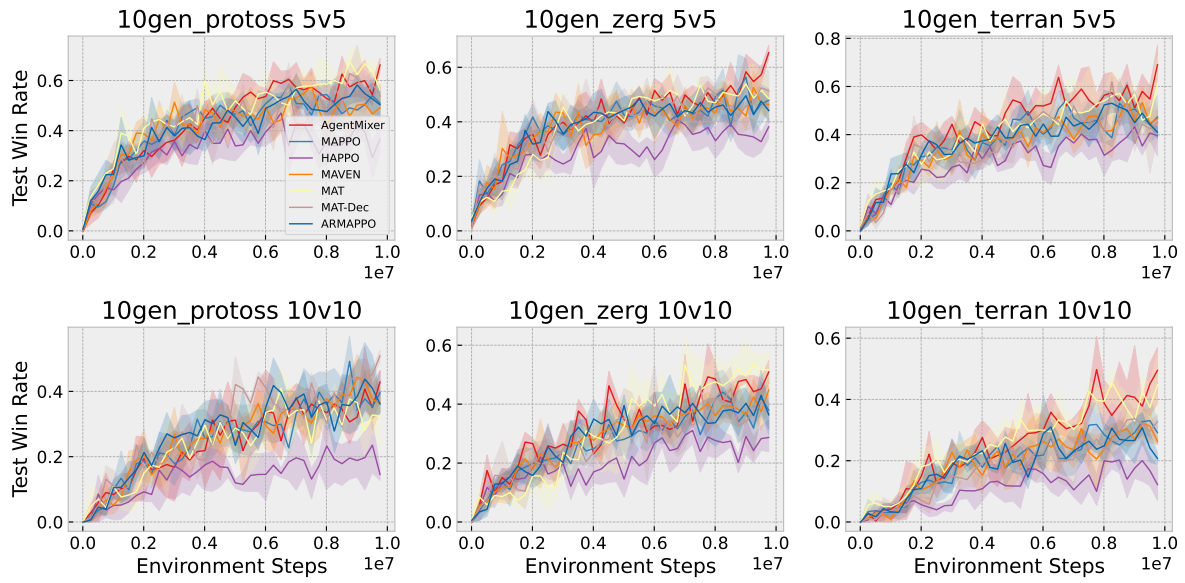


Figure 9: Comparison of the mean test win rate on SMACv2.

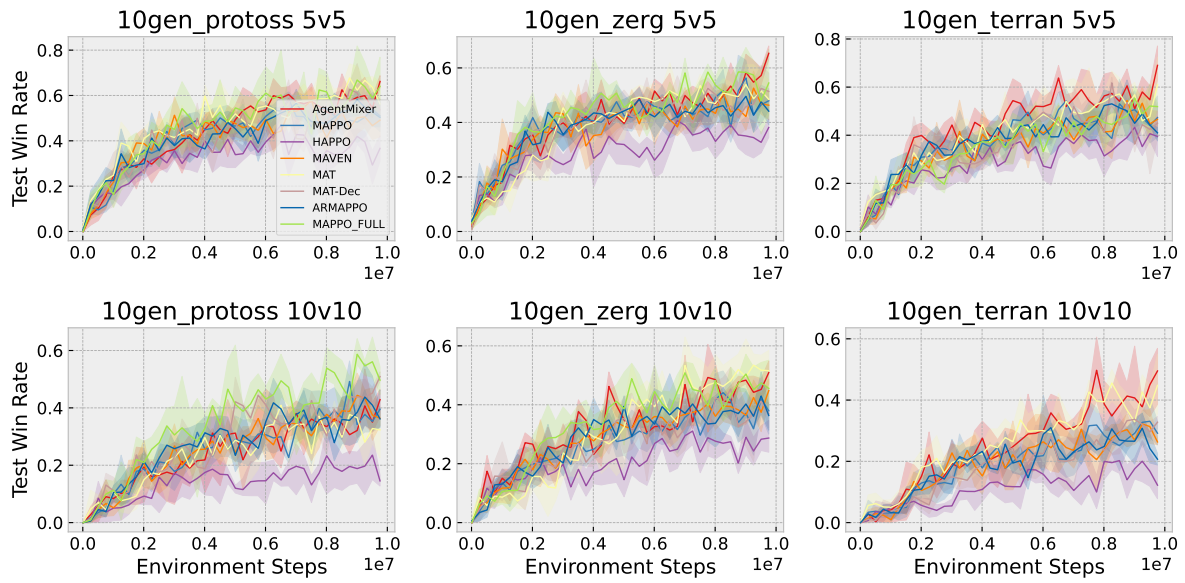


Figure 10: Ablations demonstrating the effect of full state information on SMACv2.

| Algorithm | MAPPO | HAPPO | MAT | MAT-Dec | MAVEN | ARMAPPO | AIL | Ours |
|----------------------|-------|-------|-----|---------|-------|---------|-----|------|
| P. Ob. (execution) | ✓ | ✓ | ✗ | ✗ | ✓ | ✓ | ✓ | ✓ |
| C. Value (training) | ✓ | ✓ | ✓ | ✓ | ✓ | ✓ | ✓ | ✓ |
| C. Policy (training) | ✗ | ✗ | ✗ | ✗ | ✗ | ✗ | ✓ | ✓ |

Table 2: This table compares different settings of CTDE used in baselines with our methods, where *P. Ob.* denotes *partial observation*, *C. Value* means *centralized value* and *C. Policy* represents *centralized policy*. Note that only methods with *partial observation* during execution are fair for comparison. Although all the methods take advantage of CTDE by using a *centralized value* during training, only our method and AIL further employ *centralized policy* for training. Our method tackles the *asymmetric learning failure* problem in AIL and hence shows better performance.

agents are fully independent of each other when making decisions, they may fail to coordinate their actions, which eventually leads to a sub-optimal joint policy. While with an explicit external coordination signal, MAVEN only finds the optima by chance. For MAT, since it learns a centralized auto-regressive policy, the second agent thus takes as input the first agent’s action. It is not a surprise that MAT converges to the highest return due to using a centralized policy. In contrast, thanks to the introduced IGC mechanism, AgentMixer successfully learns fully decentralized optimal policies from the optimal correlated joint policy generated by the *Policy Modifier* (PM) module.

| | | |
|-----|-----|---|
| 0 | 6 | 5 |
| -30 | 7 | 0 |
| 11 | -30 | 0 |

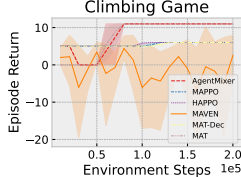


Figure 11: Left: the *Climbing* matrix game; right: the performance comparison.

More Experiments on Predator-Prey

We use an environment similar to that described by Li et al. (2020) where agents are controlled to capture prey. If a prey is captured, the agents receive a reward of 10. However, the environment penalizes any single-agent attempt to capture prey with a penalty. Note that when the penalty is non-zero, explicit coordination is needed to learn a meaningful joint policy. Figure 12 shows the average return for test episodes for varying penalties. While MAT performs best when the penalty equals zero, we should note that MAT takes an unfair full observation. In contrast, our method with partial observation outperforms all the baselines on *Penalty=-1* task which necessitates a sophisticated coordination strategy.

Ablation Study of Underlying Reinforcement Learning Algorithms

We study the impact of single-agent algorithms in Figure 13. Additional experiments confirm the universality of AgentMixer. Note the Q in AgentMixer-SAC is a centralized action-value function that takes as input the actions of all agents. In future work, we may explore integrating AgentMixer-SAC with QMix (Rashid et al. 2020).

Ablation Study of PM modules

We study the impact of different types of PM modules on SMACv2 in Table 3. The highest performance is achieved by MLP-based PM.

| Map | MLPs | Hypernetworks | Attention |
|-------------|-----------------------------|----------------------|----------------------|
| protoss 5v5 | 0.68 _{0.04} | 0.60 _{0.13} | 0.59 _{0.14} |
| terran 5v5 | 0.71 _{0.10} | 0.53 _{0.13} | 0.60 _{0.02} |
| zerg 5v5 | 0.66 _{0.03} | 0.52 _{0.08} | 0.49 _{0.10} |

Table 3: Performance comparison across different architectures.

Run Time Comparison

AgentMixer introduces additional modules that propose more computation requirements. Table 4 shows the comparison of run-time (sec) and standard deviation on the SMAC-v2 10gen_zerg scenario (steps=1e7):

Statistical Significance Test

We conducted statistical significance tests based on the T-test (Drummond and Tom 2011), using the average of the last 5 evaluations over 5 random seeds across different baselines on various benchmarks. In the tests, we set the null hypothesis as AgentMixer’s superior performance compared to other baselines is due to chance (i.e., AgentMixer’s performance is less than or equal to others).

The p-values reported in Figure 14 across various configurations (e.g., Ant-v2, HalfCheetah-v2, Humanoid-v2) consistently indicate significant results ($p < 0.05$) in favor of AgentMixer. This strongly suggests that the superior performance of AgentMixer is not a product of random variation but rather a consistent and significant improvement over the other baseline algorithms. Therefore, we conclude that AgentMixer demonstrates a robust and statistically significant advantage in performance in the MA-MuJoCo environment compared to the tested alternatives.

Hyper-parameters

For a fair comparison, the implementation of AgentMixer and the baselines are based on the implementation of MAPPO. We keep all hyper-parameters unchanged at the origin best-performing status. The proposed method and compared baselines are implemented into parameter independent version except MAT and MAT-Dec. The common

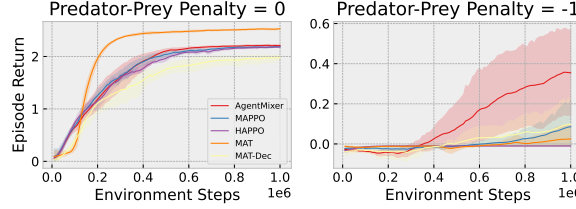


Figure 12: Performance comparison on Predator-Prey with different penalties for single-agent capture attempt.

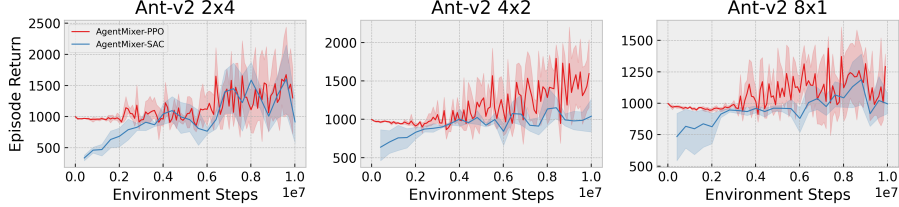


Figure 13: Impact of single-agent algorithms on AgentMixer's performance in MA-MuJoCo.

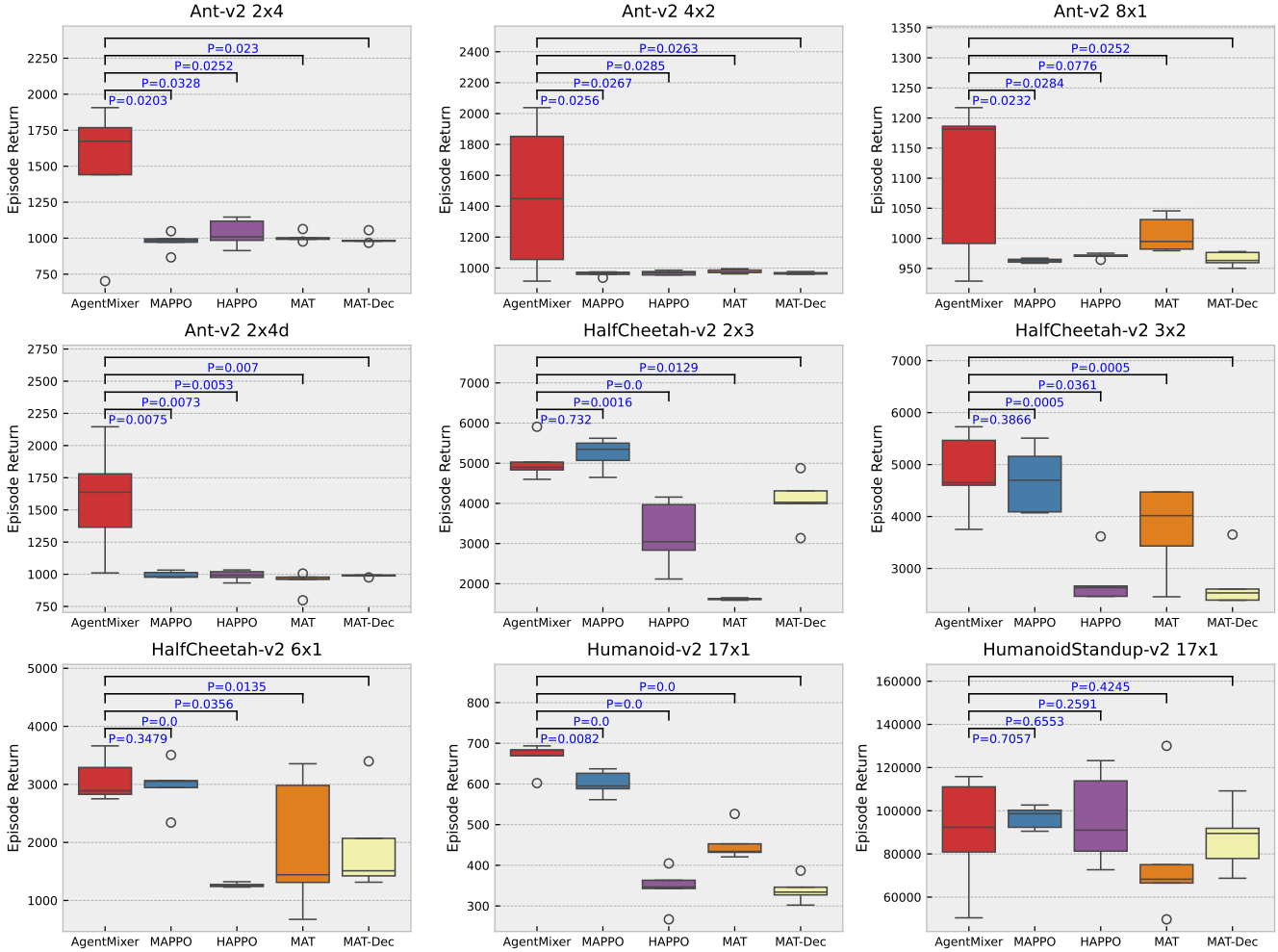


Figure 14: Statistical significance test on MA-MuJoCo. Significant results ($p < 0.05$) confirm the consistently superior performance of AgentMixer.

| Task | MAPPO | HAPPO | MAT | MAVEN | Ours |
|----------|---------------------------|--------------------------|---------------------------|---------------------------|----------------------------|
| 5 vs 5 | 19778.6 _{2927.1} | 16736 _{1270.0} | 19333.2 _{650.9} | 20883.4 _{1832.7} | 33234.6 _{4206.8} |
| 10 vs 10 | 24070 _{2130.9} | 25217.2 _{224.9} | 35758.8 _{2842.8} | 27751.6 _{966.5} | 60737.4 _{1248.62} |

Table 4: Comparison of run-time (sec) and standard deviation on the SMAC-v2 10gen_zerg scenario (steps=1e7)

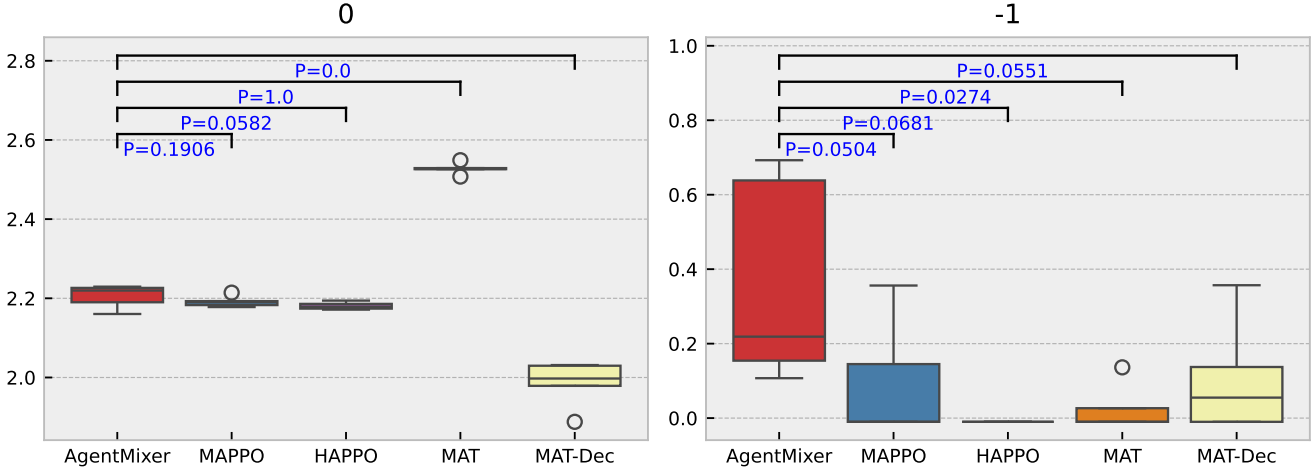


Figure 15: Statistical significance test on Predator-Prey. While MAT (oracle) achieves the best performance without penalty, it is greatly affected by non-zero penalty.

and different hyper-parameters used for the baselines and AgentMixer across all domains are listed in Table 5-11 respectively. All experiments were conducted on a cluster equipped with 10 Dell PowerEdge C4140.

Common Hyper-parameters

We list the common hyper-parameters across all the domains in Table 5-8.

| Parameter | Value |
|---------------------------|-------|
| agent-mixing hidden dim | 32 |
| channel-mixing hidden dim | 256 |
| mixer lr | 5e-5 |

Table 5: Unique hyper-parameters of AgentMixer.

| Parameter | Value |
|--------------|-------|
| block number | 1 |
| head number | 1 |

Table 6: Unique hyper-parameters of MAT / MAT-Dec.

Matrix Games

We list the hyper-parameters used in matrix games in Table 9.

SMACv2

We list the hyper-parameters used for each map of SMACv2 in Table 10.

| Parameter | Value |
|------------------------|-------|
| noise dim | 2 |
| epsilon start | 1.0 |
| epsilon end | 1.0 |
| target update interval | 200 |

Table 7: Unique hyper-parameters of MAVEN.

| Parameter | Value |
|-------------------|-------|
| Training | |
| optimizer | Adam |
| optimizer epsilon | 1e-5 |
| weight decay | 0 |
| max grad norm | 10 |
| data chunk length | 1 |
| Model | |
| activation | ReLU |
| PPO | |
| ppo-clip | 0.2 |
| gamma | 0.99 |
| gae lambda | 0.95 |

Table 8: Common hyper-parameters used across all domains.

MA-MuJoCo

The hyper-parameters used for each task of MA-MuJoCo are listed in Table 11.

| Parameter | Value |
|-------------------|--------|
| Training | |
| actor lr | 5e-4 |
| critic lr | 5e-4 |
| entropy coef | 0.01 |
| Model | |
| hidden layer | 1 |
| hidden layer dim | 64 |
| PPO | |
| ppo epoch | 15 |
| ppo-clip | 0.2 |
| num mini-batch | 1 |
| Sample | |
| environment steps | 200000 |
| rollout threads | 50 |
| episode length | 200 |

Table 9: Common hyper-parameters used in matrix games.

| Parameter | Value |
|-------------------|----------|
| Training | |
| actor lr | 5e-4 |
| critic lr | 5e-4 |
| entropy coef | 0.01 |
| Model | |
| hidden layer | 1 |
| hidden layer dim | 64 |
| PPO | |
| ppo epoch | 5 |
| ppo-clip | 0.2 |
| num mini-batch | 1 |
| Sample | |
| environment steps | 10000000 |
| rollout threads | 50 |
| episode length | 200 |

Table 10: Common hyper-parameters used in the SMACv2.

Broader Impact

We believe that the proposed work enhances the capacity for intelligent decision-making in complex and dynamic environments, and can have a positive impact on real-world multi-agent applications such as robotics, traffic management, and resource allocation. However, it is essential to consider potential concerns such as the discrepancy between the simulated environment and the real world. Another potential effect of directly implementing the derived policy is that it could lead to biased decision-making and privacy infringements. Mitigation strategies to address potential hazards could include the establishment of ethical guidelines and regulatory frameworks alongside the integration of transparency and explainability.

| Parameter | Value |
|-------------------|----------|
| Training | |
| actor lr | 3e-4 |
| critic lr | 3e-4 |
| entropy coef | 0 |
| Model | |
| hidden layer | 2 |
| hidden layer dim | 64 |
| PPO | |
| ppo epoch | 5 |
| ppo-clip | 0.2 |
| num mini-batch | 1 |
| Sample | |
| environment steps | 10000000 |
| rollout threads | 40 |
| episode length | 100 |
| Environment | |
| agent obsk | 0 |

Table 11: Common hyper-parameters used in the MA-MuJoCo.